Polymer Testing 82 (2020) 106273

Contents lists available at ScienceDirect

Polymer Testing

journal homepage: http://www.elsevier.com/locate/polytest

Material Behaviour

The effect of hot air exposure on the mechanical properties and carbon dioxide permeability of hydrogenated nitrile butadiene rubber (HNBR) with varying carbon black content

Ben Alcock [a,*], Thijs Peters [b], Avinash Tiwari [c,1]

[a] Department of Materials and Nanotechnology, SINTEF Industry, Oslo, Norway
[b] Department of Sustainable Energy Technology, SINTEF Industry, Oslo, Norway
[c] Department of Mechanical and Industrial Engineering (MTP), Norwegian University of Science and Technology, Richard Birkelands vei 2B, N-7491, Trondheim, Norway

ARTICLE INFO

Keywords:
Elastomer
Ageing
Mechanical properties
Diffusion
Permeability
Carbon dioxide

ABSTRACT

The effect of hot air exposure at 150 °C for up to 12 weeks (ca. 2000 h) on the properties of hydrogenated nitrile butadiene rubber (HNBR) compounds with varying degrees of carbon black content was investigated and reported in this paper. The composition of the HNBR was varied with 0, 10, 30 or 50 PHR carbon black. The tensile properties, hardness, density, solvent saturation swelling and carbon dioxide permeability of these specimens was investigated before and after exposure in a hot air oven. Correlations between these results are reported for the compounds considered in this work. These correlations illustrate how the changes in performance which would require test samples of specific geometries (such as tensile modulus or gas permeation) might in some cases be predicted by tests which do not require exact geometries (such as density or surface hardness), for the materials investigated in this paper.

1. Introduction

Hydrogenated nitrile butadiene rubbers (HNBRs) are commonly used in applications such as seals in oil and gas production applications due to the combination of good chemical resistance with low temperature flexibility. These elastomers may be tailored for specific applications by changing the composition such as the acrylonitrile content or additive packages, or the type and loading of fillers to achieve the desired balance of performance for the intended application. However, it is well known that the properties of elastomers such as HNBRs change once they start to be used in a service environment, during application over extended time periods [1,2], mechanical loading [3], exposure to different chemical environments [4–11], extremes of temperatures [7,12–17], irradiation (for example electron beam [18–20], ion beam [21] or gamma irradiation [22,23]) or combinations of these. Depending on the exposure conditions, these changes in properties may be attributed to increased crosslinking, molecular degradation (i.e. chain scission), main chain stiffening (e.g. by cyclization [12,24]), the absorption of chemicals from the environment or the desorption of volatile groups such as plasticizers (e.g. in Ref. [8]) or short chain segments, or most likely, combinations of these processes at various stages in the life of the elastomer. Therefore, during the service life of a component such as an elastomer o-ring or a gasket, the properties can be expected to change, and in some cases, these changes may be so significant that the function of the elastomer component is impaired, which in turn may lead to leakage or seal failure [14,25,26].

It is challenging to predict when failure may occur while an elastomer part is in service, as the fluctuations in the environment that the part has experienced may not be known, and the material properties are difficult to measure *in situ*. Therefore, elastomer parts are often retrieved and replaced according to a service schedule based on lifetime predictions (including the relevant safety factors) rather than the detection of a failure event. Retrieved elastomer parts may be damaged during retrieval and since they are perceived to have limited value, may be immediately discarded. It can be beneficial to characterise these retrieved elastomer components because the changes in properties resulting from the time exposed in the real application can provide valuable information to increase confidence in lifetime prediction for

* Corresponding author.
E-mail address: ben.alcock@sintef.no (B. Alcock).
[1] (Present address) Peter Grünberg Institute, Forschungszentrum Jülich, 52425 Jülich, Germany.

https://doi.org/10.1016/j.polymertesting.2019.106273
Received 2 August 2019; Received in revised form 27 November 2019; Accepted 1 December 2019
Available online 6 December 2019

future components. For example, the sealing force of an elastomer seal which may be used as a failure criterion linked to seal leakage, can be predicted reasonably well by correlation to compression set, as reported by Gillen et al. [27] for seals retrieved from service. However, some standardised tests may be difficult to perform on retrieved parts because the complicated or irregular geometries of worn or broken parts means that they are not usually well suited to characterisation techniques that require specific test geometries (such as tensile tests). Other techniques can be less sensitive to the test geometry (such as density testing) or may be quickly performed using portable, low cost equipment (such as shore hardness testing on flat surfaces). Therefore, it is interesting to understand how the properties which cannot be measured in complicated geometries may be estimated from the properties that can be more easily measured in retrieved pieces of end-of-life products.

One relevant elastomer property for seal performance is the way in which gases diffuse through these elastomers because, in addition to leakage around a seal [28], diffusion through the materials determines how well they can seal a gas environment. The combination of gas diffusion properties and mechanical properties affects the resistance of elastomers to rapid gas decompression (RGD) damage [29,30]. The degree of RGD damage is affected by the conditions prior to decompression such as gas type, gas pressure and the rate of decompression [31]. In addition, the mechanical properties of the elastomer also effect the resistance to RGD damage. The faster that gases can diffuse through and out of the material, the less local pressure build-up would be expected and so less RGD damage would be expected. Although RGD damage itself will not be reported in this paper, the diffusivity and solubility through compounds of HNBR is reported using carbon dioxide as a model gas. While carbon dioxide is used as a model gas to measure general gas diffusion properties, carbon dioxide storage and transport is becoming more important as part of carbon capture management strategies, and therefore understanding how elastomers behave in CO_2 environments is becoming even more important for material selection [32–35].

The elastomer compounds investigated in this paper contain the same HNBR polymer component with varying amounts of carbon black filler. These compounds are assessed before and after exposure to elevated temperature in a hot air environment as an example of an accelerated ageing process that might be expected in application, although the nature of these ageing processes is very dependent on the environment of the application. Elastomers exposed to different chemical environments may undergo different processes from those that are reported in this paper (e.g. Refs. [10,11,36,37]). To give a better overall description of changes which occur in the material resulting from hot air exposure, the mechanical properties are also reported as these will influence not only the ability of the seal to respond to strain, but also the resistance of the seal to tolerate rapid gas decompression damage. The stiffer the material, the lower local strains would be expected due to gas bubble nucleation and expansion. At the same time, the stronger the material is, the more resistant it would be expected to be to catastrophic failure due to local deformations.

In this paper, a range of HNBR compounds will be exposure to hot air and characterised after various exposure times. The mechanical properties, estimation of the apparent crosslink density (by solvent saturation swelling), thermal stability (by thermogravimetric analysis), CO_2 diffusivity and density of these specimens after different exposure times are reported. These properties will be compared to show if measurements that are less sensitive to geometry may be used as crude predictors of other characteristics. Thermal decomposition and solvent saturation swelling analyses are also including to provide information on the changes in composition and structure of the samples after exposure. Any relationships suggested in this paper are specific to the range of materials considered here, but could also be indicative of relationships in other materials although that would need to be assessed on a case by case basis.

2. Materials

Compounds with the same basic formulation of HNBR and different loadings of carbon black were made and the samples were named “0PHR”, “10PHR”, “30PHR” and “50PHR”. PHR describes the percentage mass of carbon black added relative to the mass of the polymer (HNBR) present in the compound. The formulations are shown in Table 1, and are based on compounds made and investigated in earlier studies [10,11], using HNBR with 36% acrylonitrile content and 96% saturation. Not all of the formulations were characterised with all of the techniques reported in this paper; instead research efforts were prioritised based on the samples which showed the most interesting results based on an iterative approach.

3. Experimental

3.1. Thermal exposure

The four different material formulations shown in Table 1 (HNBR with 0, 10, 30 or 50 PHR carbon black) were stamped from 2 mm thick sheets into ISO 37 Type 2 tensile specimens, which were then placed in a circulating air oven at 150 °C for 7, 24, 42 or 84 days (1, ca. 3.5, 6 and 12 weeks). In addition, 120 × 120 × 2mm plates were placed in the oven for 12 weeks to be used for gas permeation testing.

3.2. Solvent saturation swelling and density measurement

Sections of the tensile test specimens were taken to i) measure density by immersion in water and ii) perform saturation swelling experiments by immersion in chloroform. The density of the samples was measured by using the Archimedes principle; the masses of each of 3 samples were compared when immersed in either deionised water or in air. The density of the water was measured using a glass mass of calibrated volume.

Solvent saturation swelling tests were performed as follows. Different samples were immersed in chloroform and the weight gain due to swelling in chloroform was measured. The solvent absorption is used to measure the change in apparent crosslink density using formulae reported elsewhere (e.g. Ref. [11]). Three samples of selected combinations of material and exposure time were used. The samples were weighed, immersed in chloroform and reweighed periodically until the mass reached saturation. Periodic weighing during the immersion of preliminary samples showed that the mass increase after 7 days was >95% of the mass increase after up to 34 days. Therefore, these saturation swelling test results can be considered to be subject to ≤5% underestimation.

3.3. Mechanical testing

Tensile tests were performed on specimens with ISO 37 Type 2 geometry which had been exposed to up to 12 weeks in an oven at 150 °C to determine the effect of the exposure time on the tensile strength,

Table 1
The compositions of the four different materials described in this paper. All samples have the same composition except for the relative carbon black loading.

Material	Sample Name			
	0PHR	10PHR	30PHR	50PHR
HNBR	100	100	100	100
Antioxidant	3	3	3	3
Stearic Acid	0.5	0.5	0.5	0.5
Zinc Oxide	5	5	5	5
Magnesium Oxide	10	10	10	10
Plasticizer	20	20	20	20
Peroxide	10	10	10	10
N-330 HAF Carbon Black	0	10	30	50

stiffness and strain to failure. The samples were tested in a Zwick universal testing machine equipped with a 2.5 kN loadcell and a Zwick Multiextens extensometer. The samples were loaded to tensile failure at a rate of 25 mm/min. Linear extension of the sample was measured by an extensiometer, and the tensile modulus was calculated using the gradient of the curve at a strain range of 0.05–0.25% strain, after an initial preload of 0.1 N. All tests were performed at 23 °C ± 1 °C, and at least four of each specimen type was tested. Although thermal ageing is known to strongly affect the resistance of HNBR to dynamic loading [38], only quasi-static mechanical testing will be described in this paper.

In addition, Shore D hardness tests were performed on the samples comprising 3 stacked layers of 2 mm thick sheets, according to ISO 7619–1. Shore hardness is included because although it gives limited information compared to tensile testing, it is quick and easy to perform and it is commonly used for comparing and specifying elastomers for industrial applications. All hardness measurements presented in this paper are performed on surfaces which had been directly exposed to hot air. It has been reported that diffusion limited oxidation (DLO) may lead to inhomogeneous properties following hot air exposure and the degree of inhomogeneity in properties due to DLO may also depend on the service time and temperature. The elastomer surface may be more strongly affected by hot air exposure than subsurface material, and therefore surface hardness may not be representative of the hardness throughout the volume of an elastomer part [7]. Despite this drawback, surface hardness measurements were investigated here to indicate how changes in surface hardness of samples after thermal ageing might relate to changes in tensile properties, since surface hardness measurements are relatively easy to perform on samples retrieved from surface, while tensile tests which have more complex geometrical requirements, are not.

3.4. Thermogravimetric analysis

Thermogravimetric analysis (TGA) was used to measure the relative compositions of the materials after thermal exposure in the oven. 8–15 mg of each of the materials was heated in a PerkinElmer Pyris 1 TGA at 20K.min^{-1} up to 850 °C, with a 30 min isothermal hold at 850 °C, according to thermal profile A of ISO 9924–3. In this method, the initial heating is in a nitrogen atmosphere to 600 °C, and cooled down to 400 °C before changing to an air atmosphere and further heating to 850 °C, as shown in Fig. 1. The residual mass after the first stage of heating (heating to 600 °C and subsequently cooling to 400 °C in nitrogen) was used to measure the relative mass of the material pyrolised in nitrogen, and the residual mass after the isothermal hold at 850 °C was used as a measure of the ash content of the samples.

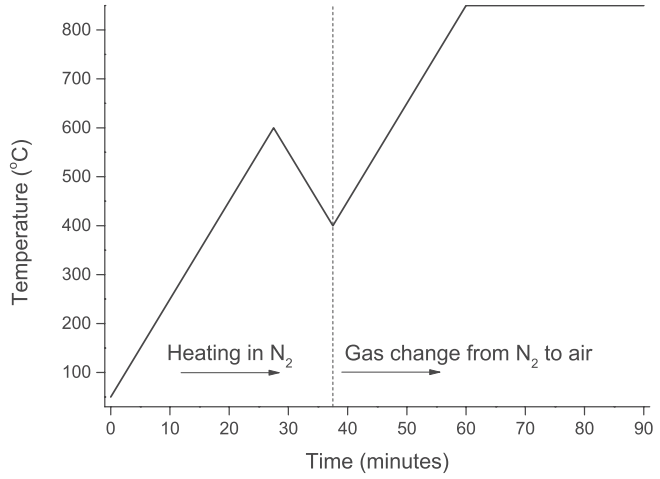

Fig. 1. The time-temperature profile used in TGA analysis.

3.5. Gas permeability

The changes in structure expected as result of the hot air exposure in the oven would be expected to affect the gas permeation through the materials. The permeation of a gas through a polymer is dependent on factors such as the free volume of the polymer, the size of the gas, the affinity for the gas to the polymer, any filler materials within the polymer, the partial pressure of the gas and the temperature at the time of permeation. CO_2 was selected as a model gas to compare these changes in permeation, which has also been investigated in similar materials which had been subjected to ageing in a hot solvent exposure in a previous study [11]. In this study, the diffusivities of samples were tested on a circular porous support of diameter 8 cm (area 50.3 cm^2). It is assumed that the porous support does not influence the measured permeation, and that there is no leakage around the specimen.

The gas permeability test process is similar to that reported in a previous study [11], but will be described here for completeness. Automated mass flow controllers (Bronkhorst High-Tech) were used to control the gas supply to either side of the HNBR sheet. The module is heated to 80 °C, with the sample in a N_2 (feed)/Ar (permeate) (99.999%) at 2 bar N_2-atmosphere until 80 °C was reached, at which point the N_2 was replaced with CO_2 (99.95%) and the pressure increased to 20 bars. The pressure of the feed side of the HNBR sheet was controlled with the help of a back pressure controller (Bronkhorst High-Tech). The volume below the HNBR sheet is flushed at a constant flow rate of argon at atmospheric pressure via a mass flow controller (Bronkhorst High-Tech) in order to remove the permeated gases from the HNBR sheet. The argon flow rate is typically set to 20 Nml/min. The CO_2 permeation flux was calculated from the measured CO_2 concentration in the permeate using the calibrated flow of argon sweep gas. For this the permeate composition was monitored by a gas chromatograph (Varian Inc., CP-4900) equipped with a thermal conductivity detector (TCD). CO_2 flux measurements were subsequently performed applying a feed pressure 20 bars, at temperatures of 80, 60 and 40 °C. After changing the temperature, the CO_2 flux is left to stabilize isothermally for 2–3 days to ensure appropriate measurement. These isothermal steps are used to measure the steady state permeability, P, at different temperatures. The initial breakthrough of the CO_2 at 80 °C allows for the determination of the diffusivity, D, at this temperature. Combining these according to Equation (1) allows for the calculation of the solubility, S, at 80 °C. It is assumed that this additional 6–9 days at 40–80 °C to complete the measurements described above does not further influence the characteristics of the HNBR, as it is not considered significant compared to the previous exposure time at 150 °C.

Equation 1

$$S = \frac{P}{D}$$

4. Results and discussion

4.1. Density

The average density of samples with varying carbon black content before and after up to 12 weeks hot air exposure at 150 °C is presented in Fig. 2. The samples increase in density with increasing filler content and with exposure time; the samples with the greatest density are those which contained 50 PHR carbon black after exposure for 12 weeks at 150 °C. The density of samples without carbon black and with 50 PHR carbon black increase on average by approximately the same amount (ca. 4%) after exposure for 12 weeks. The standard deviation of the results is shown in Fig. 2, but in almost all cases the error bars are smaller than the symbols used. Since the density is measured by immersion, the density is subject to errors due to internal porosity of the samples. Since the standard deviation of the density measurements is very small, it is assumed that either no internal porosity was present, or

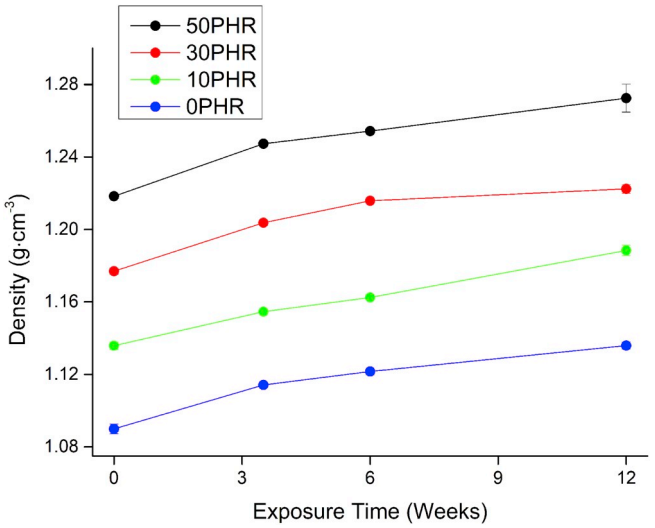

Fig. 2. The density of samples of different carbon black content after up to 12 weeks exposure to 150 °C hot air. Error bars are present but in most cases are smaller than the symbols used to show the data.

it is was consistent in all samples.

4.2. Solvent swelling

After removal of the samples from the hot air oven exposure, the mass increase due to solvent (chloroform) saturation at room temperature was measured and this is shown in Fig. 3. The samples which contain more carbon black show lower mass increases due to chloroform absorption. This can be expected since the absorption occurs in the polymer component of the compound, and samples which have a higher carbon black content have proportionally less polymer to swell. Samples which had been exposed for longer periods in hot air also show lower mass increases due to chloroform absorption, which is a reasonable expectation which may be explained by an increase in crosslink density.

In this work, HNBR samples were characterised after exposure in hot air. In a previous work [11], similar HNBR samples were exposed in a mix of solvents at elevated temperatures and pressure to simulate subsea bore use. The results of these two studies are now compared to investigate how hot air ageing compared to ageing in a solvent environment. After exposure for 12 weeks to 150 °C hot air in this work, the samples with 50 PHR carbon black reached a saturation in swelling of ca. 115% increase in mass. This is slightly less than reported previously [11] for similar samples exposed for 12 weeks in mixed solvents at the same temperature (ca. 140% increase in mass). However, the samples reported here with 50 PHR carbon black before hot air exposure also swelled slightly less (ca. 220% increase) than samples reported in our previous work [11] before hot solvent mix exposure (ca. 250% increase). This shows the same trend that the weight increase due to solvent swelling decreases with increasing exposure time at 150 °C in hot air or in a solvent mix. The discrepancy in degree of the weight increases due to solvent swelling may be due to the difference between exposure in hot air vs exposure in hot solvents, or it may simply reflect batch to batch variations in the material quality, and so this comparison is indicative but not conclusive.

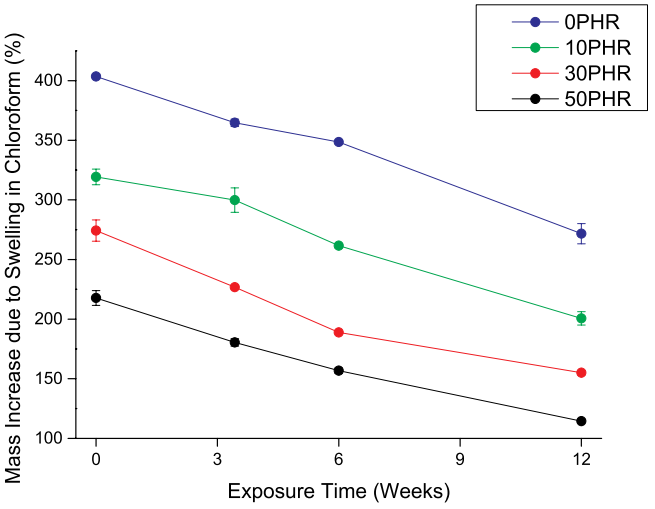

Fig. 3. The effect of hot air exposure time (at 150 °C) on the subsequent gravimetric saturation swelling of samples in chloroform, for samples with different loadings of carbon black. For clarity, a 100% mass increase represents 2x the initial mass, while a 400% mass increase represents 5x the initial mass. Error bars are present on all data points to show the standard deviation, but in most cases these error bars are smaller than the data point markers.

Based on the saturation swelling data shown in Fig. 3, the apparent degree of crosslinking in the material can be crudely estimated as described previously [11]. Fig. 4 shows M_c, an estimation of the molecular weight of material between crosslinks for samples with different carbon black loading, before and after exposure to hot air at 150 °C for 12 weeks. As the mass increase due to saturation swelling in chloroform decreases with time of exposure to hot air (Fig. 3), the estimated value of M_c decreases, i.e. there is estimated to be statistically less material between crosslinks and so the apparent crosslink density increases. It should be noted that this is estimation is indicative but ignores a number of important features of the material which would likely affect the result. In this calculation, the elastomer is modelled as a three phase system comprising elastomer, carbon black filler and swelling solvent (chloroform). In reality, as shown in Table 1, a number of additional components are present, some of which are present in particulate form in the tested elastomer samples and therefore would contribute to a reduction in mass increase due to swelling in solvent [39]. The total amount of bound rubber which is adsorbed on the surfaces of carbon black agglomerates, and is known to have less molecular freedom than rubber which is not bound to filler particles, would also likely change with carbon black content, as would rubber occluded by the agglomerates [40]. The swelling behaviour of elastomers in proximity to filler particles is known to be unrepresentative of the swelling behaviour in the bulk of the elastomer [41] and although these are likely to reduce the saturation swelling behaviour (and thus impact the crosslink density estimations), this effect is not isolated in these results. In addition, although a correction is made for the change in density of all samples

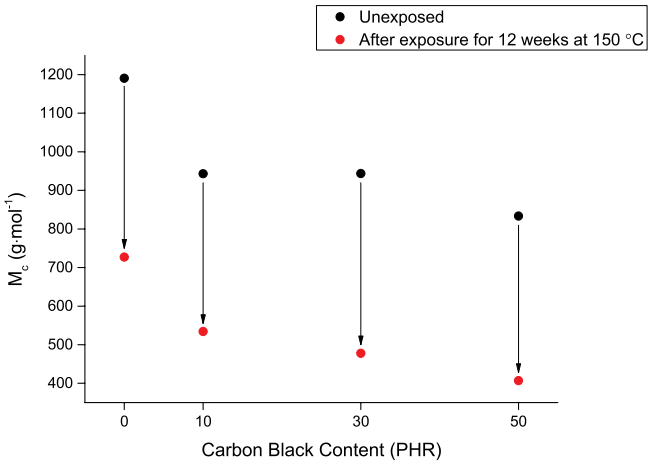

Fig. 4. The apparent molecular weight between crosslinking estimated from saturation swelling of HNBR specimens in chloroform, before and after hot air exposure for 12 weeks at 150 °C.

based on the change in density of the 0 PHR samples in Fig. 2, the exact mechanisms behind the change in density are not addressed. Factors such as evaporation of volatile species in the samples during exposure in the oven would likely affect the estimation of crosslink density as it means that the composition of the material is altered by the hot air exposure process. An increase in crosslink density may itself cause an increase in sample density resulting from a denser, more crosslinked structure and a reduction in free volume. Therefore, estimations of crosslink density of samples with different filler content and different thermal histories should be considered indicative and is not intended to very accurately describe the true density of crosslinking.

4.3. Mechanical testing

The tensile strength, stiffness and strain to failure of specimens are shown in Fig. 5, Fig. 6 and Fig. 7 respectively. There is a clear trend that tensile modulus increases with exposure time, and the effect is increased with increasing loadings of carbon black. The average tensile modulus of the unexposed specimens with 50 PHR carbon black (ca. 55 MPa) is ca. 6x higher than the average modulus of the unexposed specimens without carbon black (ca. 9 MPa). The average modulus of the specimens with 50 PHR carbon black exposed for 12 weeks (ca. 490 MPa) is ca. 12x higher than the average modulus of the unexposed specimens without carbon black exposed for the same time (ca. 40 MPa). This shows the effect of the carbon black loading on the stiffening of the material during high temperature exposure. The samples with 50 PHR have less polymer per mass than the unfilled samples and so if the change in stiffness was solely due to changes in the polymer network structure, a larger change might be expected in the unfilled samples than in the filled samples; however, this is not the case. It has been reported that the presence of carbon black interferes with the oxidation mechanisms of nitrile rubbers, with lower activation energies calculated for stiffening processes in nitrile rubbers reinforced with carbon black [42]. Fig. 8 shows the relationship between the apparent crosslink density estimated from saturation swelling in chloroform with the tensile modulus, confirming that the tensile modulus increases with decreasing saturation swelling (which is then used to estimate an increasing apparent crosslink density). The toughness of the samples, as indicated by the strain to failure (shown in Fig. 7) follows a less clear trend, as strain to failure and tensile strength are strongly influenced by defects in the material, but overall, the strain to failure decreases with increasing exposure time.

Comparing the measured density data from Fig. 2 with the tensile modulus data from Fig. 5 reveals that for these samples and exposure conditions, density appears to correlate reasonably well as a predictor of tensile modulus, as shown in Fig. 9. This is an important observation because density can be measured on irregular/small samples, and therefore can be measured quickly and easily on almost any samples retrieved from parts in service to estimate stiffness, unlike tensile stiffness measurements which require test coupons of specific geometries. While this correlation appears valid for the specimens presented in this paper, it is not known if this correlation would be also valid outside of these exposure conditions or for samples of greater filler contents.

The shore hardness of the samples is shown in Fig. 10. As would be expected based on the stiffness values shown in Fig. 5, the shore D hardness values increase with exposure time for all of the compounds, although the relationship is less clear. For all samples, there is a relatively large increase in hardness during the initial 3.5 weeks compared to the change between 3.5 and 6 weeks. This probably reflects the hardening of the rubber surface which may occur very early in the exposure process, since shore D hardness measurements are more sensitive to changes in material near the surface than deeper in the bulk of the material. In Fig. 11, these Shore D hardness values are plotted against the tensile modulus values which were presented in Fig. 5. Even though the hardness measurements focus on properties near the surface of the material, while tensile tests measure the stiffness of the entire cross-section of the specimen, the values fit reasonably well in these

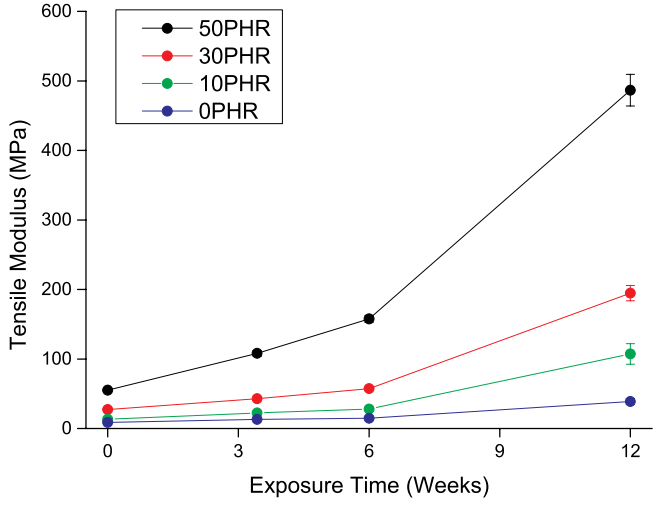

Fig. 5. The effect of hot air exposure (150 °C) on the tensile modulus, for samples with different loadings of carbon black.

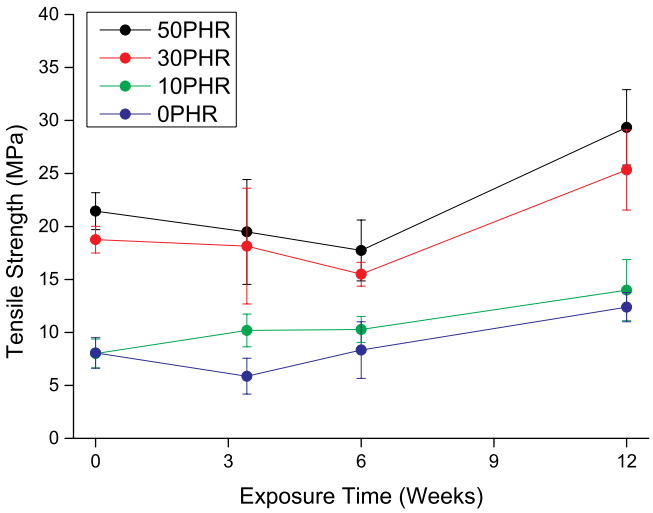

Fig. 6. The effect of hot air exposure (150 °C) on the tensile strength, for samples with different loadings of carbon black.

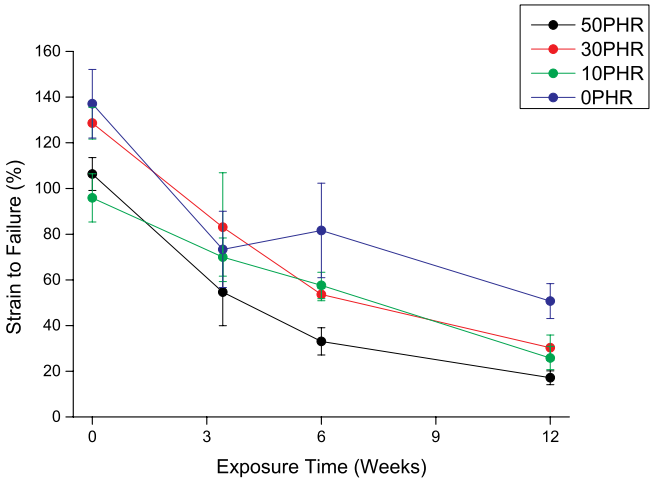

Fig. 7. The effect of hot air exposure (150 °C) on the tensile strain to failure, for samples with different loadings of carbon black.

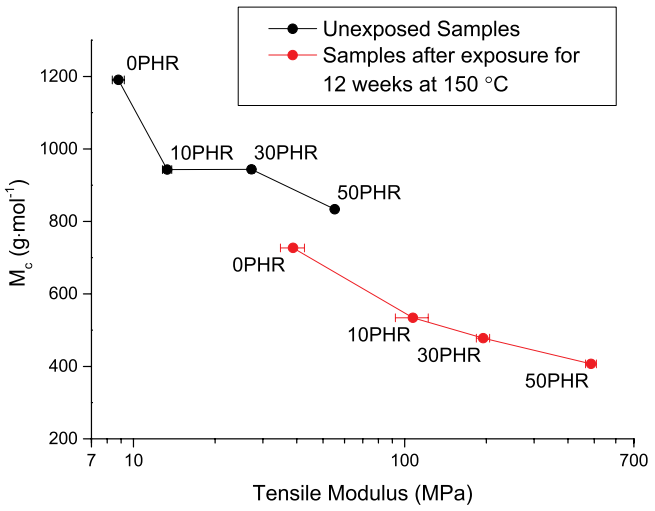

Fig. 8. The relationship between the apparent molecular weight between crosslinking estimated from saturation swelling of HNBR specimens in chloroform and the tensile modulus for the samples before or after exposure to hot air (150 °C) for 12 weeks. X axis error bars are included but are in some cases smaller than the data markers.

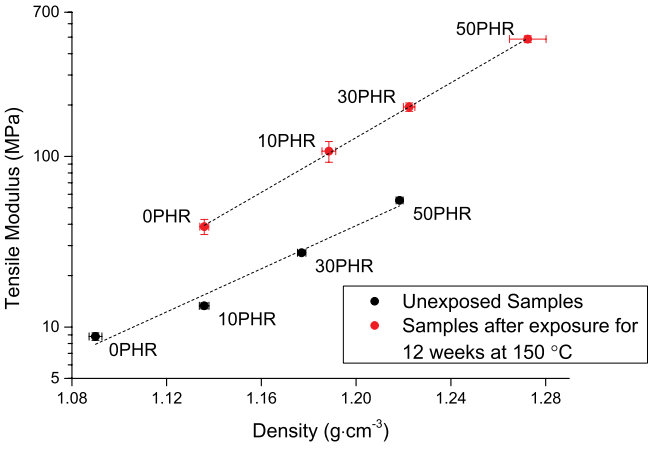

Fig. 9. The relationship between density and tensile modulus for samples before exposure or after exposure to hot air (150 °C) for 12 weeks. Dashed lines show best fit trend lines for samples exposed to the same duration in hot air ($R^2 > 0.967$ in all cases). Error bars are included in both axes but are in most cases smaller than the data markers.

ranges on shore D hardness. This is similar to work previously reported by Mix and Giacomin [43] and others. While the combined values fit a good general trend in this set of data, the data for all material types fit slight curves with larger increases in hardness at lower stiffnesses. This relationship may simply be due to slight non-linearity in the hardness vs. tensile modulus relationship in this range of samples. It may also include a contribution from a diffusion limited oxidation effect, although that may be limited since these samples are quite thin. The surface material which has contact to the hot air during oven exposure would be expected to harden faster than the material inside of the samples at shorter exposure times, while the material deeper under the surface would be expected to be affected more slowly (due to the need for diffusion of oxygen into the sample). Since the tensile modulus is a measure of the average stiffness in the cross section of a test specimen, while hardness is a measurement of the surface material, it is reasonable that the hardness shows an more rapid increase after shorter exposure times and then a slower increase after longer exposure times, while the modulus increases more steadily with exposure time. In any case, this shows that although

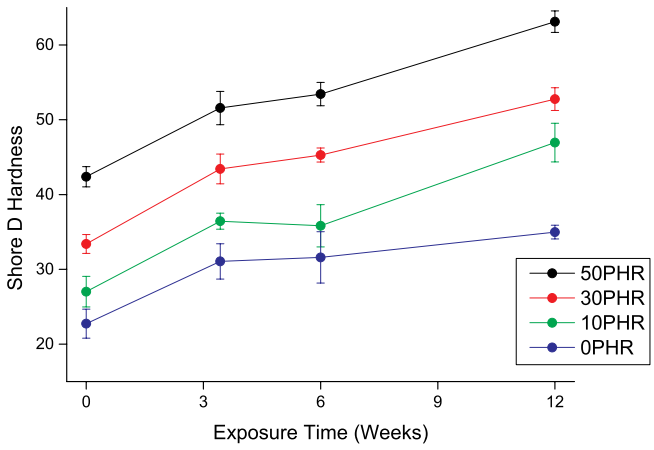

Fig. 10. The effect of hot air exposure (150 °C) on the shore D hardness, for samples with different loadings of carbon black.

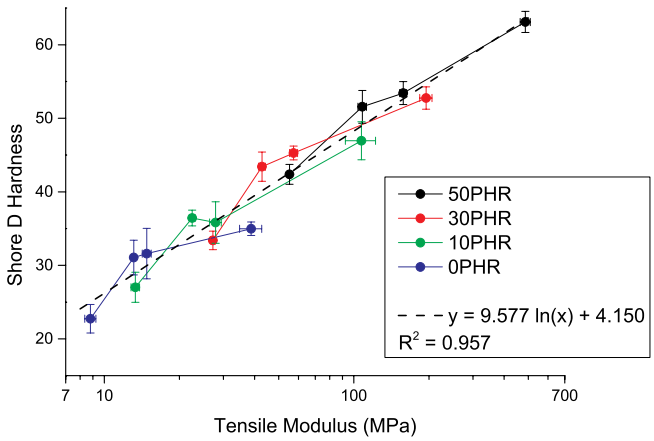

Fig. 11. The relationship between shore D hardness and tensile modulus for samples with different carbon black loadings which have been exposed to hot air exposure (150 °C) for different durations. A best fit (dashed) trend line which reasonably well describes all the data points is included, although each data set for the different carbon black loadings appears to fit slightly curved trends for each material formulation, as shown by the lines linking the data points.

hardness and tensile stiffness may be compared in homogenous samples, the situation may be more complicated with samples which show surface to bulk inhomogeneity, especially in parts with increasing volume to surface ratios.

4.4. Thermogravimetry

Thermogravimetric weight loss curves of samples without carbon black before and after 3.5 or 12 weeks exposure to hot air at 150 °C are shown in Fig. 12. Negligible weight loss is seen in the samples before they reach ca. 400 °C, with a dramatic mass loss between 400 and 500 °C before reaching ca. 15–20% of the initial mass at 600 °C in nitrogen. The samples which had been exposed in the oven at 150 °C for 12 weeks show higher residual mass at this point than those which had not been exposed. The samples are then cooled to 400 °C, and the gas is changed from nitrogen to air, and then heated from 400 °C to 800 °C. In this final heating in air, all the samples reached the same residual mass by approximately 550 °C.

Thermogravimetric weight loss curves of samples with 50 PHR carbon black before and after exposure to 1–12 weeks in hot air at 150 °C are shown in Fig. 13. These carbon black filled samples show the same

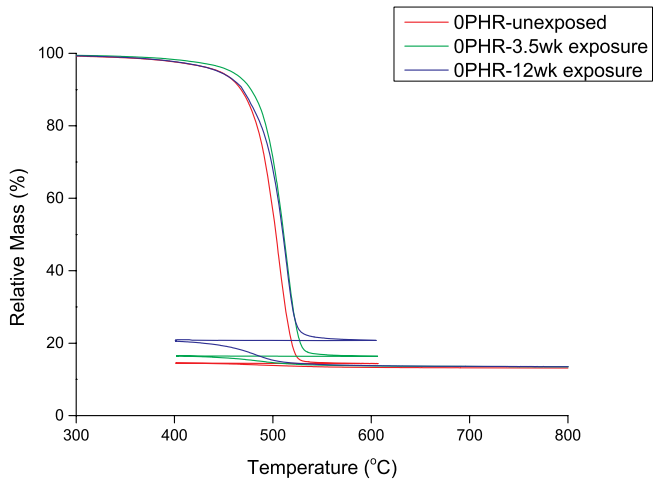

Fig. 12. The effect of hot air exposure (150 °C) on the thermogravimetric analysis of samples without carbon black before exposure, and after 3.5 and 12 weeks exposure.

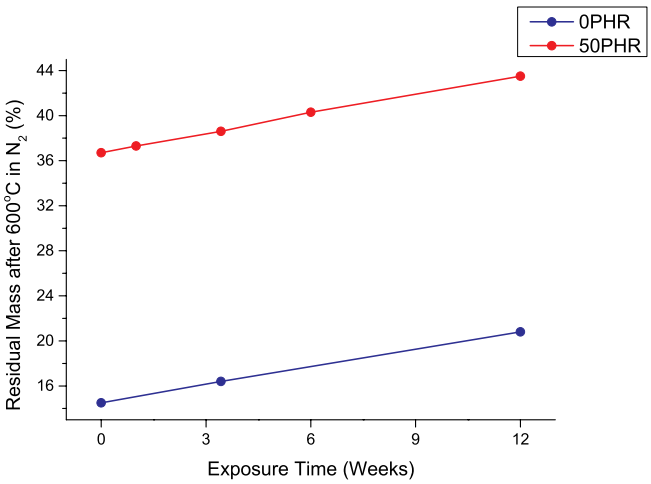

Fig. 14. The relationship between the residual mass after heating to 600 °C in a nitrogen atmosphere and the hot air exposure time at 150 °C, for samples with 0 or 50 PHR carbon black.

general behaviour as the unfilled samples shown in Fig. 12; the longer the exposure time, the higher the residual mass after the initial heating to 600 °C in a nitrogen atmosphere in the TGA. Since there is a smaller proportion of polymer present in these carbon black filled samples, these samples do not show such a large initial decrease in mass when heating in nitrogen to 600 °C. Upon switching from nitrogen to an air atmosphere at 400 °C, and heating to 800 °C, the samples with the longest oven exposure times show the earliest mass loss although all samples with the same composition ultimately reach the same final relative mass irrespective of ageing time in the oven. Fig. 14 shows that relationship between the residual mass after heating to 600 °C in a nitrogen atmosphere for samples with 0 and 50 PHR carbon black and the exposure time at 150 °C has an approximately linear trend.

During the initial pyrolysis in the nitrogen atmosphere, it is likely that carbonaceous residues are built up in the HNBR samples [44,45], as this is expected for elastomers containing nitrogen [46]. As described by ISO 9924–3, these may oxidise soon after switching to an air atmosphere in the second stage of a two stage thermogravimetric analysis, and this corresponds to what is seen in Figs. 12 and 13. Fig. 14 shows that the amount of residual mass after heating to 600 °C in nitrogen increases with the exposure time in the oven at 150 °C, even though the total volumes of pyrolysable polymer relative to the combusted carbon black and final mineral contents remain constant in Fig. 13. This may reflect cyclization of the ACN groups during the exposure at 150 °C [12,24], yielding structures which are both thermally stable and would be expected to contribute to the increase in stiffness and hardness of the structure, as seen in Figs. 5 and 10, and possibly also to the reduction in saturation swelling as seen in Fig. 3.

4.5. Carbon dioxide permeation

The permeability of samples of varying carbon black content which were either unexposed or had been exposed for 12 weeks at 150 °C are shown in Fig. 15 at permeation test temperatures of 40, 60 or 80 °C. This shows that for all of these samples, the permeability increases with diffusion test temperature (as reported before for similar samples which had been aged by exposure to a solvent mix instead in hot air [11]). This decrease in CO_2 permeability with ageing in hot air follows the same trends as the decrease in oxygen permeability reported previously by Kömmling et al. [7]. Assuming one effect is an increase in crosslink density with exposure time, the decrease in permeability is as may be expected based on molecular models of HNBR with varying increasing crosslink density [47,48]. The permeability also decreases with

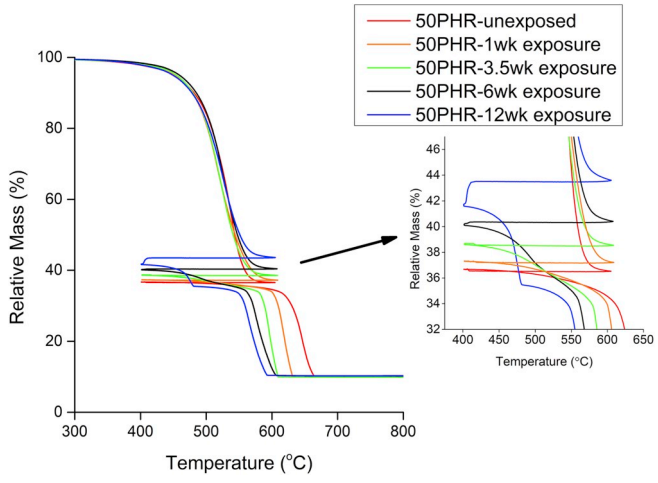

Fig. 13. The effect of hot air exposure (150 °C) on the thermogravimetric analysis of samples with 50 PHR carbon black. Inset: magnified view of curves immediately after switch of gas from nitrogen to air at 400 °C.

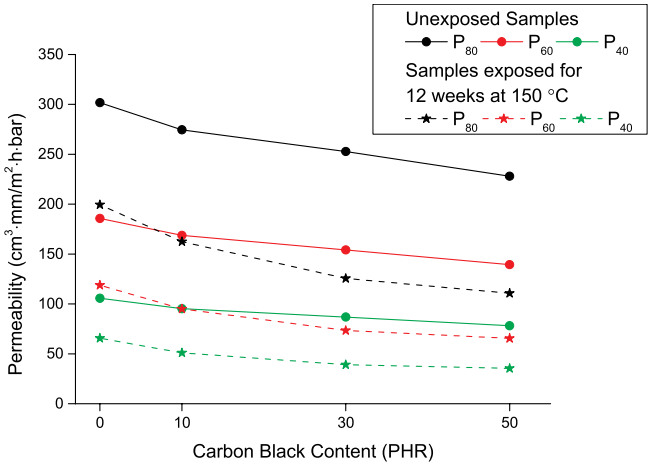

Fig. 15. The relationship between permeability and carbon black content for samples which were either unexposed or had been exposed for 12 weeks at 150 °C. The permeability is shown at three different diffusion test temperatures: 40, 60 and 80 °C.

increasing carbon black content, presumably because the increasing content of carbon black agglomerates functions as a barrier to gas diffusion. This barrier effect due to particle inclusions would be expected to be much more efficient if a platelet shaped fillers oriented normal to the gas permeation direction were used [49,50], although this is not explored here. Fig. 16 shows the permeability at all diffusion test temperatures and illustrates that the permeability is much higher before exposure. The permeability at all diffusion test temperatures for all samples is approximately 45–66% permeability after exposure compared to before exposure. The samples with most carbon black (50 PHR) show the lowest relative change in permeability (45–49% of unexposed permeability after exposure) and the samples without carbon black (0 PHR) show the greatest relative change (62–66% of unexposed permeability after exposure). Before and after exposure, the samples with most carbon black (50 PHR) had 54–56% of the permeability of the samples without carbon black (0 PHR).

Fig. 17 shows the difference in diffusivity at 80 °C, and the difference in solubility at 80 °C for the samples before and after exposure for 12 weeks at 150 °C, with 0, 10, 30 and 50 PHR carbon black. As expected from the previous results, the diffusivity of the all of the materials decreases after 12 weeks of hot air exposure in the oven, and the greatest change is seen in the samples with 50 PHR carbon black which show a diffusivity decrease of more than 60% at 80 °C. As the density of the samples was seen to increase after exposure to hot air (see Fig. 2) it is reasonable to expect that the diffusivity would also decrease. There is no significant trend in the changes in solubility identified, suggesting that the changes in permeability are mainly related to changes in diffusivity during exposure in hot air. Fig. 18 shows the relationship between density (at 20 °C) and diffusivity (at 80 °C) which closely fit trendlines indicating that density measurements at room temperature may be used to predict diffusivity of these specimens at higher temperatures. As described earlier for the relationship between tensile stiffness and density (Fig. 9), the use of density measurements to predict diffusivity may allow estimations of diffusivity of samples of irregular geometry, such as in parts retrieved from service. However, the observed correlations presented here should be considered to be limited to the materials investigated in this paper after the reported hot air exposure durations.

5. Conclusions

A range of HNBR compounds with differing carbon black contents were characterised after varying durations of exposure in a hot air oven at 150 °C. The effect on the mechanical properties, composition and gas permeability and diffusivity is reported. The tensile stiffness increased

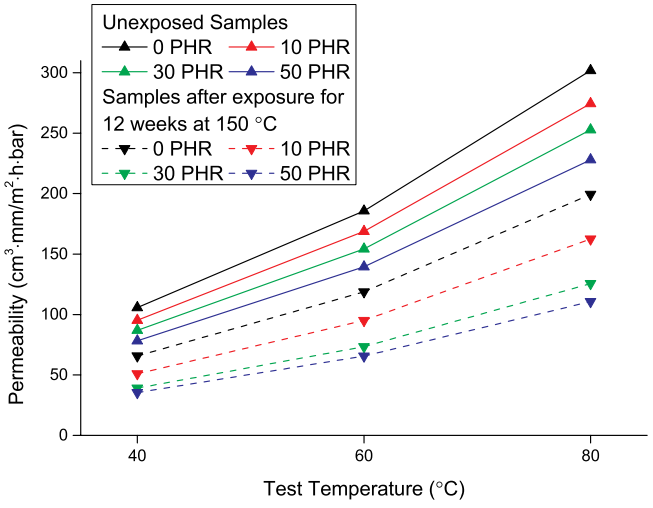

Fig. 16. The relationship between permeability and test temperature for samples which were either unexposed or had been exposed for 12 weeks at 150 °C.

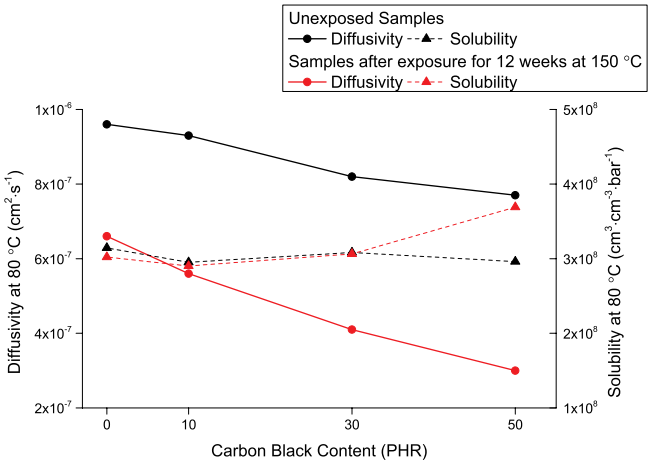

Fig. 17. The relationship between diffusivity at 80 °C and carbon black content, and solubility at 80 °C and carbon black content for samples which were either unexposed or had been exposed for 12 weeks at 150 °C.

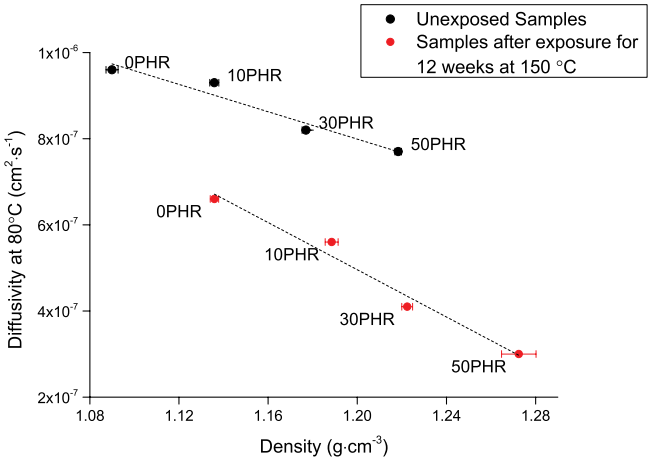

Fig. 18. The relationship between density (at 20 °C) and diffusivity (at 80 °C) for samples before exposure or after exposure to hot air (150 °C) for 12 weeks. Dashed lines show best fit trend lines for unexposed samples ($R^2 = 0.947$) and samples after exposure to hot air for 12 weeks ($R^2 = 0.976$). Error bars in density are included but are in most cases smaller than the data markers.

while the samples became more brittle with increasing exposure time. The effect of exposure time on tensile strength was less clear. The effect on exposure time on the tensile modulus was strongest with greatest carbon black content. Shore hardness increased non-linearly with tensile modulus. A correlation was shown between tensile stiffness and density in these samples, illustrating how measurements of changes in density may be used as a way to predict changes in stiffness in samples which are not available in a shape suitable for tensile testing. Material inhomogeneities which would be expected to result from the hot air exposure (for example by diffusion limited oxidation) were not explicitly considered here.

Thermogravimetry suggests a build-up of carbonaceous material during hot air exposure. During subsequent TGA analysis, this is stable in nitrogen but pyrolised in air upon a switch of test gas. This demonstrates the importance of analytical thermogravimetry under different gas environments.

Diffusion studies using CO_2 as a model gas reveals how the permeability (at different temperatures) and diffusivity (at 80 °C) decrease due to hot air exposure of the HNBR samples. As expected, the samples with the greatest carbon black content provided the best barriers to CO_2 diffusion. As with tensile stiffness, changes in density appear to trend

well with changes in diffusivity which may mean that density could be used as a quick and easy predictor of diffusivity for these materials, if the composition is known. The decrease in diffusivity with hot air exposure suggests that the elastomers investigated here would become more efficient in gas barrier seal applications after exposure to elevated temperatures. However, this improvement in gas barrier performance (i.e. reduced diffusion through the seal) must be balanced with the stiffening of the elastomer which could lead to greater leakage *around* the seals.

Data availability

The raw/processed data required to reproduce these findings cannot be shared at this time as the data also forms part of an ongoing study.

Declaration of competing interest

The authors declare that they have no known competing financial interests or personal relationships that could have appeared to influence the work reported in this paper.

CRediT authorship contribution statement

Ben Alcock: Conceptualization, Investigation, Methodology, Resources, Supervision, Project administration, Writing - original draft, Writing - review & editing, Resources. **Thijs Peters:** Methodology, Investigation, Formal analysis, Writing - original draft, Writing - review & editing. **Avinash Tiwari:** Conceptualization, Methodology, Resources, Writing - review & editing.

Acknowledgements

This work is part of the collaborative project "Thermo Responsive Elastomer Composites for cold climate application" with the industrial partners FMC Kongsberg Subsea AS, STATOIL Petroleum AS, the Norwegian University of Science and Technology (NTNU) and the research institute SINTEF Industry. The authors would like to express their thanks for the financial support by the Research Council of Norway (Project 234115 in the Petromaks2 programme). The authors are also grateful Marius Johansen at SINTEF Industry for performing the mechanical tests reported here.

Appendix A. Supplementary data

Supplementary data to this article can be found online at https://doi.org/10.1016/j.polymertesting.2019.106273.

References

[1] R.P. Brown, G. Soulagnet, Microhardness profiles on aged rubber compounds, Polym. Test. 20 (2001) 295–303.
[2] M.J. Forrest, Chemical analysis of rubber samples that had been naturally aged for 40 years, Polym. Test. 20 (2001) 151–158.
[3] Z. Zhu, C. Jiang, Q. Cheng, J. Zhang, S. Guo, Y. Xiong, B. Fu, W. Yang, H. Jiang, Accelerated aging test of hydrogenated nitrile butadiene rubber using the time–temperature–strain superposition principle, RSC Adv. 5 (2015) 90178–90183.
[4] C.-b. Cong, C.-c. Cui, X.-y. Meng, S.-j. Lu, Q. Zhou, Degradation of hydrogenated nitrile-butadiene rubber in aqueous solutions of H2S or HCl, Chem. Res. Chin. Univ. 29 (2013) 806–810.
[5] W. Balasooriya, B. Schrittesser, G. Pinter, T. Schwarz, Induced material degradation of elastomers in harsh environments, Polym. Test. 69 (2018) 107–115.
[6] E.A. Khorova, G.I. Razdyakonova, S.Y. Khodakova, Effect of the structure of hydrogenated butadiene-nitrile rubber on the resistance to aggressive media and high temperatures, Procedia Eng. 152 (2016) 556–562.
[7] A. Kömmling, M. Jaunich, D. Wolff, Effects of heterogeneous aging in compressed HNBR and EPDM O-ring seals, Polym. Degrad. Stab. 126 (2016) 39–46.
[8] X. Liu, J. Zhao, R. Yang, R. Iervolino, S. Barbera, Thermal aging of hydrogenated nitrile rubber – loss of additives and its influence on elasticity maintenance, Polimery 62 (2017) 588–598.
[9] W. Lou, W. Zhang, T. Jin, X. Liu, W. Dai, Synergistic effects of multiple environmental factors on degradation of hydrogenated nitrile rubber seals, Polymers (2018) 10.
[10] B. Alcock, J.K. Jørgensen, The mechanical properties of a model hydrogenated nitrile butadiene rubber (HNBR) following simulated sweet oil exposure at elevated temperature and pressure, Polym. Test. 46 (2015) 50–58.
[11] B. Alcock, T.A. Peters, R.H. Gaarder, J.K. Jørgensen, The effect of hydrocarbon ageing on the mechanical properties, apparent crosslink density and CO2 diffusion of a hydrogenated nitrile butadiene rubber (HNBR), Polym. Test. 47 (2015) 22–29.
[12] N. Verdier, D. Lepage, A. Prébé, D. Aymé-Perrot, M. Dollé, D. Rochefort, Crosslinker free thermally induced crosslinking of hydrogenated nitrile butadiene rubber, J. Polym. Sci. A Polym. Chem. 56 (2018) 1825–1833.
[13] F.-Z. Li, M.-R. Gao, B. Guo, Investigation of ageing behaviour of nitrile-butadiene rubber with added graphene in an accelerated thermal ageing environment, Kemija u Industriji 67 (2018) 29–37.
[14] A. Kömmling, M. Jaunich, P. Pourmand, D. Wolff, U.W. Gedde, Influence of ageing on sealability of elastomeric O-rings, Macromol. Symp. (2017) 373.
[15] W. Balasooriya, B. Schrittesser, S. Karunakaran, S. Schlögl, G. Pinter, T. Schwarz, Z. Kadar, Influence of thermo-oxidative ageing of HNBR in oil field applications, Macromol. Symp. 373 (2017) 1600093.
[16] B. Alcock, K. Olafsen, J. Huse, F. Grytten, The low temperature crystallization of hydrogenated nitrile butadiene rubber (HNBR), Polym. Test. 66 (2018) 228–234.
[17] S. Bhattacharjee, A.K. Bhowmick, B.N. Avasthi, Degradation of hydrogenated nitrile rubber, Polym. Degrad. Stab. 31 (1991) 71–87.
[18] S. Perraud, M.-F. Vallat, M.-O. David, J. Kuczynski, Network characteristics of hydrogenated nitrile butadiene rubber networks obtained by radiation crosslinking by electron beam, Polym. Degrad. Stab. 95 (2010) 1495–1501.
[19] P.K. Das, A. Ganguly, M. Banerji, Electron-beam curing of hydrogenated acrylonitrile–butadiene rubber, J. Appl. Polym. Sci. 97 (2005) 648–651.
[20] J. Bik, W. Głuszewski, W.M. Rzymski, Z.P. Zagórski, EB radiation crosslinking of elastomers, Radiat. Phys. Chem. 67 (2003) 421–423.
[21] N. Roche, P. Heuillet, C. Janin, P. Jacquot, Mechanical and tribological behavior of HNBR modified by ion implantation, influence of aging, Surf. Coat. Technol. 209 (2012) 58–63.
[22] W. Zhao, L. Yu, X. Zhong, Y. Zhang, J. Sun, Radiation vulcanization of hydrogenated acrylonitrile butadiene rubber (HNBR), J. Appl. Polym. Sci. 54 (1994) 1199–1205.
[23] C.P. Porter, R. Edge, M.D. Ogden, Polymeric seal degradation in nuclear power plants: effect of gamma radiation on sealing properties, J. Appl. Polym. Sci. 134 (2017).
[24] M. Giurginca, T. Zaharescu, Thermo-oxidative degradation of some polymer couples containing HNBR, Polym. Bull. 49 (2003) 357–362.
[25] P.R. Morrell, M. Patel, A.R. Skinner, Accelerated thermal ageing studies on nitrile rubber O-rings, Polym. Test. 22 (2003) 651–656.
[26] A. Kömmling, M. Jaunich, P. Pourmand, D. Wolff, M. Hedenqvist, Analysis of O-ring seal failure under static conditions and determination of end-of-lifetime criterion, Polymers 11 (2019) 1251.
[27] K.T. Gillen, R. Bernstein, M.H. Wilson, Predicting and confirming the lifetime of o-rings, Polym. Degrad. Stab. 87 (2005) 257–270.
[28] A.G. Akulichev, A.T. Echtermeyer, B.N.J. Persson, Interfacial leakage of elastomer seals at low temperatures, Int. J. Press. Vessel. Pip. 160 (2018) 14–23.
[29] M. Najipoor, L. Haroonabadi, A. Dashti, Assessment of failures of nitrile rubber vulcanizates in rapid gas decompression (RGD) testing: effect of physico-mechanical properties, Polym. Test. 72 (2018) 377–385.
[30] L. Haroonabadi, A. Dashti, M. Najipour, Investigation of the effect of thermal aging on rapid gas decompression (RGD) resistance of nitrile rubber, Polym. Test. 67 (2018) 37–45.
[31] B. Schrittesser, G. Pinter, T. Schwarz, Z. Kadar, T. Nagy, Rapid Gas Decompression Performance of elastomers – a study of influencing testing parameters, Procedia Struct. Integr. 2 (2016) 1746–1754.
[32] X. Chen, H.A. Salem, R. Zonoz, CO_2 solubility and diffusivity and rapid gas decompression resistance of elastomers containing CNT, Rubber Chem. Technol. 90 (2017) 562–574.
[33] D. Zhu, Y. Lin, H. Ma, H. Zhang, Y. Li, L. Zhang, K. Deng, Experimental studies on CO2 corrosion of rubber materials for packer under compressive stress in gas wells, Eng. Fail. Anal. 80 (2017) 11–23.
[34] E. Lainé, J.C. Grandidier, G. Benoit, B. Omnès, F. Destaing, Effects of sorption and desorption of CO2 on the thermomechanical experimental behavior of HNBR and FKM O-rings - influence of nanofiller-reinforced rubber, Polym. Test. 75 (2019) 298–311.
[35] L. Ansaloni, B. Alcock, T.A. Peters, Effects of CO2 on polymeric materials in the CO2 transport chain: a review, Int. J. Greenh. Gas Contr. 94 (2020). https://doi.org/10.1016/j.ijggc.2019.102930.
[36] W. Lou, W. Zhang, X. Liu, W. Dai, D. Xu, Degradation of hydrogenated nitrile rubber (HNBR) O-rings exposed to simulated servo system conditions, Polym. Degrad. Stab. 144 (2017) 464–472.
[37] W. Lou, W. Zhang, H. Wang, T. Jin, X. Liu, Influence of hydraulic oil on degradation behavior of nitrile rubber O-rings at elevated temperature, Eng. Fail. Anal. 92 (2018) 1–11.
[38] K.N. Ulu, B. Huneau, E. Verron, P. Heuillet, A.-S. Béranger, Fatigue of HNBR blends and the effects of thermal ageing, Procedia Eng. 213 (2018) 153–160.
[39] A.N. Gent, J.A. Hartwell, G. Lee, Effect of carbon black on crosslinking, Rubber Chem. Technol. 76 (2003) 517–532.
[40] J.-B. Donnet, E. Custodero, Reinforcement of elastomers by particulate fillers, in: J. E. Mark, B. Erman, C.M. Roland (Eds.), The Science and Technology of Rubber, 2013.

[41] J.J.C. Busfield, A.G. Thomas, K. Yamaguchi, Electrical and mechanical behavior of filled elastomers 2: the effect of swelling and temperature, J. Polym. Sci. B Polym. Phys. 42 (2004) 2161–2167.
[42] M. Celina, J. Wise, D.K. Ottesen, K.T. Gillen, R.L. Clough, Oxidation profiles of thermally aged nitrile rubber, Polym. Degrad. Stab. 60 (1998) 493–504.
[43] A. Mix, A. Giacomin, Standardized polymer durometry, J. Test. Eval. 39 (2011) 696–705.
[44] C.J. Norris, M. Hale, M. Bennett, Composition and property changes of HNBR and FKM elastomers after sour gas aging, Plast. Rubber Compos. 45 (2016) 239–246.
[45] A.K. Sircar, Analysis of elastomer vulcanizate composition by TG-DTG techniques, Rubber Chem. Technol. 65 (1992) 503–526.
[46] D.W. Brazier, Applications of thermal analytical procedures in the study of elastomers and elastomer systems, Rubber Chem. Technol. 53 (1980) 437–511.
[47] N. Molinari, M. Khawaja, A.P. Sutton, A.A. Mostofi, Molecular model for HNBR with tunable cross-link density, J. Phys. Chem. B 120 (2016) 12700–12707.
[48] M.M. Khawaja, Modelling the Permeability of Nitrile Rubber - PhD Thesis, The Department of Physics, Imperial College, London, 2016.
[49] X. Yang, U. Giese, R.H. Schuster, Characterization of Permeability of Elastomers: Part I HNBR, KGK Kautschuk Gummi Kunststoffe, 2008, pp. 294–300.
[50] M. Klüppel, M.M. Möwes, A. Lang, J. Plagge, M. Wunde, F. Fleck, C.W. Karl, Characterization and application of graphene nanoplatelets in elastomers, in: K. W. Stöckelhuber, A. Das, M. Klüppel (Eds.), Designing of Elastomer Nanocomposites: from Theory to Applications, Springer International Publishing, Cham, 2017, pp. 319–360.